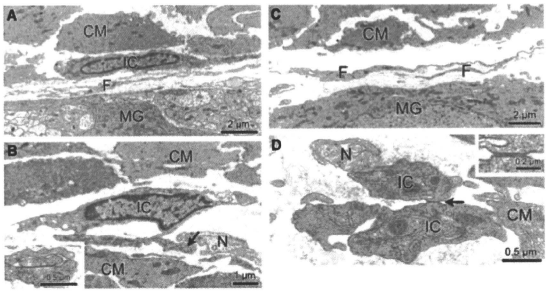

Figure 6 (A–B) Morphology of the tunica muscularis from the corpus of a sham-operated rat. (A) Electron micrographs of the myenteric plexus region. Typical ICC-MY (IC) were observed near the myenteric ganglion (MG), significantly different in appearance from fibroblasts (F). (B) ICC-IM (IC) are closely associated with nerve fivers (N) and shared gap junctions (arrow) with adjacent ICC-IM. Inset: Higher magnification of a gap junction is indicated by the arrow. (C–D) Morphology of the tunica muscularis from the corpus of an I/R rat. (C) Electron micrographs of the myenteric plexus region. Only fibroblasts were observed as the interstitial cells around the myenteric ganglion, and no ICC were observed. (D) The remaining ICC-IM showed the same ultrastructure as that in the sham-operated rats and shared gap junctions (arrow) with adjacent ICC-IM. Inset: Higher magnification of a gap junction indicated by the arrow.

accelerated gastric emptying. However, decreased expression of nNOS in the pyloric sphincter might more potently contribute to the delayed gastric emptying through blockage of the passage of liquid through the pyloric ring (Fig. 5), and a combination of these events might have resulted in a moderate delay of gastric emptying observed after gastric I/R. Transient focal cerebral ischaemia in rats can cause severe damage to nNOS-positive neurons and their eventual death.[30] In the present study, a minor, albeit significant decrease in PGP9.5-positive neurons was observed in the corpus after I/R, suggesting possible damage to enteric neurons. However, we did not detect any cell death by the terminal deoxynucleotidyl transferase-mediated dUTP nick end labelling (TUNEL) method (data not shown), and the reduced expression of nNOS was shown to be restored by 48 h after I/R, suggesting differential effects of I/R on nNOS-positive neurons in the stomach and cerebrum. Proteins, including PGP9.5, in the nNOS-positive neurons might have been transiently downregulated after I/R in the corpus. As hypoxia has been reported to rather increase nNOS expression,[31] the reduction of nNOS expression after I/R observed in the present study might have occurred in the reperfusion stage. I/R-induced production and release of proinflammatory interferon-γ[32] and platelet-activating factor[33] might contribute to the reduced expression of nNOS.[34,35]

In the present study, concomitant decrease in the number of nNOS and ICC was observed in the corpus at 12 h, and then restored at 48 h after I/R (Figs 3 and 4). According to the report by Choi *et al.*,[36] significant reduction of the c-Kit immunoreactive networks of ICC from nNOS-deficient mice was observed as compared with that in the control mice and the number of ICC in organotypic cultures increased by an NO donor and decreased by an NOS inhibitor, suggesting that nNOS-derived NO is important for the presence of ICC in the gastrointestinal tract. In contrast, the distribution of NOS-containing nerves were unaffected by the absence of ICC in W/W^v animals.[37] Thus, reduction in the number of nNOS-positive neurons might be involved in the loss of ICC in the corpus after I/R. However, as the lack of temporal correlation between the reduced nNOS and c-Kit expression has been reported in non-obese diabetic (NOD) mice,[38] a common factor might have induced the simultaneous loss of both the ICC and nNOS-positive neurons. Oxidative stress produced by the xanthine–xanthine oxidase system after I/R may have played a major role in the disruption of the ICC network in this model, as oxidative stress associated with diabetes has been reported to induce a reduction of c-Kit expression and ICC damage.[38] Disruption of the ICC in the antrum persisted until 48 h after I/R, at which point the nNOS expression was restored. It appears that the recovery of the ICC network in the antrum might take longer as compared with that in the corpus. The decrease in the expression of membrane-bound SCF at 12 and 48 h after I/R in the present study (Fig. 2) might have also contributed to the delayed recovery of the ICC in the antrum, as reported for studies of diabetic *db/db* mice and NOD mice,[39,40] although the contribution might have been small in this acute model of gastric I/R. The

differential effect of I/R on the ICC in the corpus and antrum still remains to be elucidated.

The ultrastructural analysis revealed a marked decrease in the number of cells with typical ICC morphology at 12 h after I/R (Fig. 6). These results indicate that the reduction in c-Kit protein observed after I/R probably reflected true loss of ICC. Apoptosis of ICC has been reported to be detected after intestinal ischaemia for 60 min and reperfusion for 12 h by TUNEL method. [41] However, we did not detect apoptosis by the same method after gastric ischaemia for 80 min and reperfusion for 12 h and no characteristic findings of cell death were detected by electron microscopy. There is a possibility that the apoptotic ICC were already phagocytozed by 12 h after I/R in the stomach. However, since the ICC in the corpus were restored by 48 h after I/R, it is unlikely that the gastric ICC undergo apoptosis after gastric I/R. According to a previous report, under the condition of blockade of the c-Kit pathway, the ICC phenotype changes toward a more smooth muscle-like phenotype.[42] In the present study, we did not detect any intermediate phenotype by electron microscopy at 12 h after I/R. Although the ICC might have undergone complete transition to smooth muscle cells, further investigation is awaited to clarify the exact fate of the ICC after I/R.

In conclusion, delayed gastric emptying was observed after gastric I/R, with a significant decrease in the number of ICC and nNOS-positive neurons. These results suggest that the rat model of gastric ischaemia and reperfusion is a convenient model of acute gastroparesis that shows a similar pathology to diabetic gastroparesis.

CONFLICT OF INTEREST

No conflicts of interest exist.

REFERENCES

1 Kitajima M, Otsuka S, Shimizu A *et al.* Impairment of gastric microcirculation in stress. *J Clin Gastroenterol* 1988; **10**(Suppl. 1): S120–8.

2 Zinner MJ, Turtinen L, Gurll NJ. The role of acid and ischemia in production of stress ulcers during canine hemorrhagic shock. *Surgery* 1975; **77**: 807–16.

3 Takeuchi K, Ueshima K, Hironaka Y, Fujioka Y, Matsumoto J, Okabe S. Oxygen free radicals and lipid peroxidation in the pathogenesis of gastric mucosal lesions induced by indomethacin in rats. Relation to gastric hypermotility. *Digestion* 1991; **49**: 175–84.

4 Suzuki H, Hibi T, Marshall BJ. Helicobacter pylori: present status and future prospects in Japan. *J Gastroenterol* 2007; **42**: 1–15.

5 Suzuki H, Suzuki M, Imaeda H, Hibi T. *Helicobacter pylori* and microcirculation. *Microcirculation* 2009; **16**: 547–58.

6 Udassin R, Eimerl D, Schiffman J, Haskel Y. Postischemic intestinal motility in rat is inversely correlated to length of ischemia. An *in vivo* animal model. *Dig Dis Sci* 1995; **40**: 1035–8.

7 Takahashi A, Tomomasa T, Kaneko H *et al.* Intestinal motility in an *in vivo* rat model of intestinal ischemia-reperfusion with special reference to the effects of nitric oxide on the motility changes. *J Pediatr Gastroenterol Nutr* 2001; **33**: 283–8.

8 Shimojima N, Nakaki T, Morikawa Y *et al.* Interstitial cells of Cajal in dysmotility in intestinal ischemia and reperfusion injury in rats. *J Surg Res* 2006; **135**: 255–61.

9 Huizinga JD, Thuneberg L, Kluppel M, Malysz J, Mikkelsen HB, Bernstein A. W/kit gene required for interstitial cells of Cajal and for intestinal pacemaker activity. *Nature* 1995; **373**: 347–9.

10 Ward SM, Burns AJ, Torihashi S, Sanders KM. Mutation of the proto-oncogene c-kit blocks development of interstitial cells and electrical rhythmicity in murine intestine. *J Physiol* 1994; **480** (Pt 1): 91–7.

11 Torihashi S, Ward SM, Sanders KM. Development of c-Kit-positive cells and the onset of electrical rhythmicity in murine small intestine. *Gastroenterology* 1997; **112**: 144–55.

12 Ward SM, Harney SC, Bayguinov JR, McLaren GJ, Sanders KM. Development of electrical rhythmicity in the murine gastrointestinal tract is specifically encoded in the tunica muscularis. *J Physiol* 1997; **505**(Pt 1): 241–58.

13 Sanders KM. A case for interstitial cells of Cajal as pacemakers and mediators of neurotransmission in the gastrointestinal tract. *Gastroenterology* 1996; **111**: 492–515.

14 Burns AJ, Lomax AE, Torihashi S, Sanders KM, Ward SM. Interstitial cells of Cajal mediate inhibitory neurotransmission in the stomach. *Proc Natl Acad Sci USA* 1996; **93**: 12008–13.

15 Ward SM, Beckett EA, Wang X, Baker F, Khoyi M, Sanders KM. Interstitial cells of Cajal mediate cholinergic neurotransmission from enteric motor neurons. *J Neurosci* 2000; **20**: 1393–403.

16 He CL, Soffer EE, Ferris CD, Walsh RM, Szurszewski JH, Farrugia G. Loss of interstitial cells of cajal and inhibitory innervation in insulin-dependent diabetes. *Gastroenterology* 2001; **121**: 427–34.

17 Watkins CC, Sawa A, Jaffrey S *et al.* Insulin restores neuronal nitric oxide synthase expression and function that is lost in diabetic gastropathy. *J Clin Invest* 2000; **106**: 373–84.

18 Ordog T, Takayama I, Cheung WK, Ward SM, Sanders KM. Remodeling of networks of interstitial cells of Cajal in a murine model of diabetic gastroparesis. *Diabetes* 2000; **49**: 1731–9.

19 Iwasaki H, Kajimura M, Osawa S *et al.* A deficiency of gastric interstitial cells of Cajal accompanied by decreased expression of neuronal nitric oxide synthase and substance P in patients with type 2 diabetes mellitus. *J Gastroenterol* 2006; **41**: 1076–87.

20 Wang XY, Huizinga JD, Diamond J, Liu LW. Loss of intramuscular and submuscular interstitial cells of Cajal and associated enteric nerves is related to decreased gastric emptying in streptozotocin-induced diabetes. *Neurogastroenterol Motil* 2009; **21**: 1095–e92.
21 Takahashi T. Pathophysiological significance of neuronal nitric oxide synthase in the gastrointestinal tract. *J Gastroenterol* 2003; **38**: 421–30.
22 Babbedge RC, Bland-Ward PA, Hart SL, Moore PK. Inhibition of rat cerebellar nitric oxide synthase by 7-nitro indazole and related substituted indazoles. *Br J Pharmacol* 1993; **110**: 225–8.
23 Mashimo H, Kjellin A, Goyal RK. Gastric stasis in neuronal nitric oxide synthase-deficient knockout mice. *Gastroenterology* 2000; **119**: 766–73.
24 Kido T, Nakai Y, Kase Y *et al.* Effects of rikkunshi-to, a traditional Japanese medicine, on the delay of gastric emptying induced by N[G]-nitro-L-arginine. *J Pharmacol Sci* 2005; **98**: 161–7.
25 Iseri SO, Gedik IE, Erzik C *et al.* Oxytocin ameliorates skin damage and oxidant gastric injury in rats with thermal trauma. *Burns* 2008; **34**: 361–9.
26 Shea-Donohue T, Steel L, Montcalm-Mazzilli E, Dubois A. Aspirin-induced changes in gastric function: role of endogenous prostaglandins and mucosal damage. *Gastroenterology* 1990; **98**: 284–92.
27 Sykora J, Malan A, Zahlava J *et al.* Gastric emptying of solids in children with *H. pylori*-positive and *H. pylori*-negative non-ulcer dyspepsia. *J Pediatr Gastroenterol Nutr* 2004; **39**: 246–52.
28 Chiloiro M, Russo F, Riezzo G *et al.* Effect of *Helicobacter pylori* infection on gastric emptying and gastrointestinal hormones in dyspeptic and healthy subjects. *Dig Dis Sci* 2001; **46**: 46–53.
29 Wood JG, Yan ZY, Zhang Q, Cheung LY. Ischemia-reperfusion increases gastric motility and endothelin-1-induced vasoconstriction. *Am J Physiol* 1995; **269**: G524–31.
30 Sakuma M, Hyakawa N, Kato H, Araki T. Time dependent changes of striatal interneurons after focal cerebral ischemia in rats. *J Neural Transm* 2008; **115**: 413–22.
31 Ward ME, Toporsian M, Scott JA *et al.* Hypoxia induces a functionally significant and translationally efficient neuronal NO synthase mRNA variant. *J Clin Invest* 2005; **115**: 3128–39.
32 Osman M, Russell J, Granger DN. Lymphocyte-derived interferon-gamma mediates ischemia-reperfusion-induced leukocyte and platelet adhesion in intestinal microcirculation. *Am J Physiol Gastrointest Liver Physiol* 2009; **296**: G659–63.
33 Yoshikawa T, Takahashi S, Naito Y *et al.* Effects of a platelet-activating factor antagonist, CV-6209, on gastric mucosal lesions induced by ischemia-reperfusion. *Lipids* 1992; **27**: 1058–60.
34 Bandyopadhyay A, Chakder S, Rattan S. Regulation of inducible and neuronal nitric oxide synthase gene expression by interferon-gamma and VIP. *Am J Physiol* 1997; **272**: C1790–7.
35 Qu XW, Wang H, Rozenfeld RA, Huang W, Hsueh W. Type I nitric oxide synthase (NOS) is the predominant NOS in rat small intestine. Regulation by platelet-activating factor. *Biochim Biophys Acta* 1999; **1451**: 211–7.
36 Choi KM, Gibbons SJ, Roeder JL *et al.* Regulation of interstitial cells of Cajal in the mouse gastric body by neuronal nitric oxide. *Neurogastroenterol Motil* 2007; **19**: 585–95.
37 Ward SM, Morris G, Reese L, Wang XY, Sanders KM. Interstitial cells of Cajal mediate enteric inhibitory neurotransmission in the lower esophageal and pyloric sphincters. *Gastroenterology* 1998; **115**: 314–29.
38 Choi KM, Gibbons SJ, Nguyen TV *et al.* Heme oxygenase-1 protects interstitial cells of Cajal from oxidative stress and reverses diabetic gastroparesis. *Gastroenterology* 2008; **135**: 2055–64, 2064 e2051–2052.
39 Yamamoto T, Watabe K, Nakahara M *et al.* Disturbed gastrointestinal motility and decreased interstitial cells of Cajal in diabetic db/db mice. *J Gastroenterol Hepatol* 2008; **23**: 660–7.
40 Horvath VJ, Vittal H, Lorincz A *et al.* Reduced stem cell factor links smooth myopathy and loss of interstitial cells of cajal in murine diabetic gastroparesis. *Gastroenterology* 2006; **130**: 759–70.
41 Mei F, Guo S, He YT *et al.* Apoptosis of interstitial cells of Cajal, smooth muscle cells, and enteric neurons induced by intestinal ischemia and reperfusion injury in adult guinea pigs. *Virchows Arch* 2009; **454**: 401–9.
42 Torihashi S, Nishi K, Tokutomi Y, Nishi T, Ward S, Sanders KM. Blockade of kit signaling induces transdifferentiation of interstitial cells of cajal to a smooth muscle phenotype. *Gastroenterology* 1999; **117**: 140–8.

JNM J Neurogastroenterol Motil, Vol. 16 No. 1 January, 2010
DOI: 10.5056/jnm.2010.16.1.97
Journal of Neurogastroenterology and Motility

Journal Club

Post-infectious Functional Dyspepsia - A Novel Disease Entity among Functional Gastrointestinal Disorders - Relation to *Helicobacter pylori* Infection?

(Neurogastroenterol Motil 2009;21:832-e56)

Hidekazu Suzuki, M.D., Ph.D.
Division of Gastroenterology and Hepatology, Department of Internal Medicine, Keio University School of Medicine, Tokyo, Japan

Summary

Kindt et al.[1] published a report entitled "Intestinal immune activation in presumed post-infectious functional syspepsia" in the August issue of Neurogastroenterology and Motility in 2009. By comparing the signs of inflammation and the degree of hyperplasia of the enterochromaffin cells (EC) in duodenal biopsies obtained from patients with presumed post-infectious functional dyspepsia (PI-FD) and unspecified-onset functional dyspepsia (U-FD), they showed that PI-FD is associated with persistence of focal T-cell aggregates, decrease in $CD4^+$ cells and increased macrophage counts surrounding the crypts, without any significant differences in the numbers of EC or chromogranin A (CA)-positive cells (mast cells). This finding may indicate impaired ability of the immune system in these cases to terminate the inflammatory response after an acute insult.

Comment

In irritable bowel syndrome (IBS), a post-infectious disease entity was reported in 1962 by Chaudhary and Truelove, who showed that 23% of IBS patients gave a history of an episode of bacillary or amoebic dysentery.[2] Ever since, an increasing number of studies have reported on the development of post-infectious IBS.

In relation to PI-FD, Mearin et al.[3] reported a significantly increased prevalence of FD up to 1 year after an outbreak of Salmonella gastroenteritis. In PI-FD patients, early satiety, weight loss, nausea, and vomiting are more frequently reported, while gastric sensorimotor function testing revealed a particularly high prevalence of impaired gastric accommodation.[4] In the study by Kindt et al.,[1] the focal aggregates of $CD8^+$ T cells, decrease in $CD4^+$ T cells and increased macrophage counts surrounding the duodenal crypts persisted for several months after the acute infectious episodes, suggesting delay or impairment of termination of the inflammatory response even after adequate re-

Received: November 17th, 2009 Accepted: November 24th, 2009

*Correspondence: Hidekazu Suzuki, M.D., Ph.D.
Department of Internal Medicine, Keio University School of Medicine, 35 Shinanomachi, Shinjuku-ku, Tokyo 160-8582, Japan
Tel: +81-3-5363-3914, Fax: +81-3-5363-3967, E-mail: hsuzuki@sc.itc.keio.ac.jp
Financial support: This study was supported by the Keio Gijuku Academic Development Funds (to H.S.).
Conflicts of interest: None.

moval of the infecting pathogen.

Why did Kindt et al. choose duodenal mucosa over gastric biopsies for the histopathological evaluation in the FD patients? As is well known, FD symptoms are mainly attributable to disturbed gastric function. However, the approach of studying inflammation in the duodenum has been used previously[5] and in fact, was reported to be more successful for detecting the changes in FD as compared to gastric biopsies.[6] According to the report by Lee et al.,[7] since duodenal acidification induces proximal gastric relaxation, increases the sensitivity to gastric distension, and inhibits gastric accommodation to a meal, duodenal mucosa is also an important sensory portion for the pathogenesis of FD. Furthermore, when histological inflammation is assessed by gastric biopsy, we have to bear in mind the possible co-existence of *Helicobacter pylori* (*H. pylori*) infection of the stomach. Even though the Rome III classification does not require ruling out of *H. pylori* infection for diagnosing FD,[8,9] the *H. pylori*-colonized gastric mucosa exhibits significant levels of inflammatory cell infiltration with $CD8^+$-, $CD4^+$-T cells and macrophages.[10-13] Even after the eradication of *H. pylori*, many mononuclear cells as T cells or macrophages persist in the mucosa. Such inflammatory changes present before and even after *H. pylori* eradication could play a significant role in the pathophysiology of this type of dyspepsia. Taken together, functional dyspepsia with a present or even past history of *H. pylori* infection should be considered as a different disease entity from FD, such as *H. pylori*-infectious FD or post-*H. pylori*-infectious FD.

In conclusion, the concept of PI-FD is potentially valid and the causal relationship between remnant inflammatory features and the gastroduodenal motor or sensory machinery should be further investigated. However, the major microorganism infecting the stomach, *H. pylori*, should not be overlooked when considering the pathophysiology of FD, especially in Asia.

References

1. Kindt S, Tertychnyy A, de Hertogh G, Geboes K, Tack J. Intestinal immune activation in presumed post-infectious functional dyspepsia. Neurogastroenterol Motil 2009;21:832-e56.
2. Chaudhary NA, Truelove SC. The irritable colon syndrome. A study of the clinical features, predisposing causes, and prognosis in 130 cases. Q J Med 1962;31:307-322.
3. Mearin F, Pérez-Oliveras M, Perello A, et al. Dyspepsia and irritable bowel syndrome after a Salmonella gastroenteritis outbreak: one-year follow-up cohort study. Gastroenterology 2005;129:98-104.
4. Tack J, Demedts I, Dehondt G, et al. Clinical and pathophysiological characteristics of acute-onset functional dyspepsia. Gastroenterology 2002;122:1738-1747.
5. Collins JS, Hamilton PW, Watt PC, Sloan JM, Love AH. Quantitative histological study of mucosal inflammatory cell densities in endoscopic duodenal biopsy specimens from dyspeptic patients using computer linked image analysis. Gut 1990;31:858-861.
6. Collins JS, Hamilton PW, Watt PC, Sloan JM, Love AH. Superficial gastritis and *Campylobacter pylori* in dyspeptic patients--a quantitative study using computer-linked image analysis. J Pathol 1989;158:303-310.
7. Lee KJ, Vos R, Janssens J, Tack J. Influence of duodenal acidification on the sensorimotor function of the proximal stomach in humans. Am J Physiol Gastrointest Liver Physiol 2004;286:G278-G284.
8. Tack J, Talley NJ, Camilleri M, et al. Functional gastroduodenal disorders. Gastroenterology 2006;130:1466-1479.
9. Suzuki H, Nishizawa T, Hibi T. Therapeutic strategies for functional dyspepsia and the introduction of the Rome III classification. J Gastroenterol 2006;41:513-523.
10. Suzuki H, Masaoka T, Miyazawa M, Suzuki M, Miura S, Ishii H. Gastric mucosal response to *Helicobacter pylori*. Keio J Med 2002;51(suppl 2):40-44.
11. Suzuki H, Hibi T, Marshall BJ. *Helicobacter pylori*: present status and future prospects in Japan. J Gastroenterol 2007;42:1-15.
12. Suzuki H, Iwasaki E, Hibi T. *Helicobacter pylori* and gastric cancer. Gastric Cancer 2009;12:79-87.
13. Suzuki H, Suzuki M, Imaeda H, Hibi T. *Helicobacter pylori* and microcirculation. Microcirculation 2009;16:547-558

Journal of Gastroenterology and Hepatology

JGHF

doi:10.1111/j.1440-1746.2010.06245.x

ORIGINAL ARTICLE

Homology model of the DNA gyrase enzyme of *Helicobacter pylori*, a target of quinolone-based eradication therapy

Juntaro Matsuzaki, Hidekazu Suzuki, Hitoshi Tsugawa, Toshihiro Nishizawa and Toshifumi Hibi

Division of Gastroenterology and Hepatology, Department of Internal Medicine, Keio University School of Medicine, Tokyo, Japan

Key words
DNA gyrase, *Helicobacter pylori*, quinolones.

Accepted for publication 17 December 2009.

Correspondence
Dr Hidekazu Suzuki, Division of Gastroenterology and Hepatology, Department of Internal Medicine, Keio University School of Medicine, 35 Shinanomachi, Shinjuku-ku, Tokyo 160-8582, Japan. Email: hsuzuki@sc.itc.keio.ac.jp

Conflict of interest
The authors declare no conflicts of interests.

Abstract

Background and Aims: Resistance of *Helicobacter pylori* to the standard therapeutic antimicrobial agents has been demonstrated. Although quinolones are an alternative candidate for third-line eradication therapy, quinolone resistance of *H. pylori* is also increasing. Quinolone resistance of *H. pylori* is caused by a point mutation of the DNA gyrase subunit A (GyrA) protein, especially on amino acids 87 and 91. The aim of this study is to surmise the structure of *H. pylori* GryA.

Methods: The modeling of the 3-D structure of *H. pylori* GyrA was performed by an automated homology modeling program: SWISS-MODEL. The position of amino acids 87 and 91 in *H. pylori* GyrA was plotted on the homology model. To estimate the function of quinolone resistance-determining region (QRDR), the structure of *H. pylori* GyrA was compared with *Escherichia coli* GyrA.

Results: A molecular model of *H. pylori* GyrA could be predicted using SWISS-MODEL. The GyrA N- and C-terminal domains closely resembled those of *E. coli*. The position of amino acids 87 and 91 in *H. pylori* GyrA was part of the DNA binding region (head dimer interface) on the GyrA N-terminal domain.

Conclusion: Our homology model of *H. pylori* GryA suggests that the quinolone resistance-determining region is on the head dimer interface of the GyrA N-terminal domain.

Introduction

Because *Helicobacter pylori* infection is linked to peptic ulcer disease and gastric cancer,[1–5] eradication is an important preventive measure. However, increasing bacterial resistance to clarithromycin and metronidazole is compromising the eradication of *H. pylori* and causing failures in therapy.[6,7] One of the alternative candidates for third-line therapy is quinolones.[8–13] Quinolones show marked activity against *H. pylori*, as well as having good oral absorption and no major side-effects.[14] A recent *in vitro* study showed synergistic effects of quinolones and PPI against *H. pylori* strains.[15]

Quinolones exert their antimicrobial activity by inhibiting the enzyme, DNA gyrase,[16] which introduces negative supercoils into the DNA (Fig. 1). DNA gyrase is involved in DNA replication, recombination and transcription. The bacterial enzyme, gyrase, is a tetramer consisting of two A and two B subunits encoded by the *gyrA* and *gyrB* genes, respectively. The resistance of *H. pylori* to quinolones is caused by point mutations in the so-called quinolone resistance-determining region (QRDR) of the *gyrA* gene,[17,18] mainly involving amino acid substitutions at amino acid 87 (Asn to Lys) and amino acid 91 (Asp to Gly, Asp to Asn, and Asp to Tyr).[19,20]

The aim of this study was to predict the structure of *H. pylori* GryA and the function of the QRDR. This will help to determine the mechanism of the quinolone resistance of *H. pylori*, and to develop new drugs to overcome the resistance.

Methods

The modeling of the 3-D structure of *H. pylori* GyrA was performed by an automated homology modeling program: SWISS-MODEL.[21–23] SWISS-MODEL workspace[24] can be freely accessed at http://swissmodel.expasy.org/workspace/. We used the automatic modeling mode, and applied the protein sequence of *H. pylori* GyrA, which is available in GenBank (AAA74376.1). Obtained data of the homology model was visualized using DeepView ver. 4.0.1 (The Swiss Institute of Bioinformatics). The structure was compared with the structure of *Escherichia coli*'s GyrA N-terminal domain[25] (Protein Data Bank [PDB] code: 1ab4) and GyrA C-terminal domain[26] (PDB code: 1zi0B), which were also visualized using DeepView. The positions of amino acids 87 and 91 of *H. pylori* were plotted on the homology model.

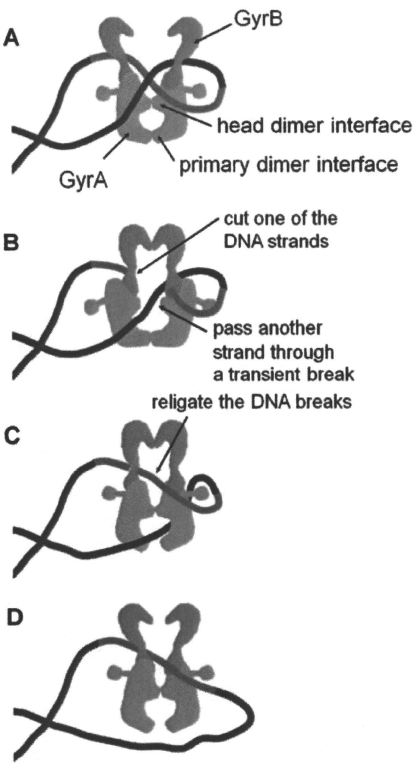

Figure 1 Function of DNA gyrase. (a) DNA gyrase is composed of two GyrA and two GyrB subunits. The two GyrA can bind at each primary dimer interface and head dimer interface. (b) DNA gyrase introduces a double-stranded break in the DNA. Another segment of DNA passes through the break to the opposite side of DNA gyrase. (c) The break in the strands is repaired. (d) One positive supercoil of DNA molecule is disentangled.

Results

According to GenBank (AAA74376.1), *H. pylori* GyrA consisted of 826 amino acids. Amino acids 37–497, which correspond to the *H. pylori* GyrA N-terminal domain, were based on the crystal structure of the topoisomerase IV subunit A (GrlA) from *Staphylococcus aureus* (PDB code: 2inrA). Amino acids 504–800, which correspond to the *H. pylori* GyrA C-terminal domain, were based on X-ray crystallography of the GyrA C-terminal domain from *E. coli* (PDB code: 1zi0B). The homology model of the *H. pylori* GyrA N-terminal domain closely resembled the crystal structure of the *E. coli* GyrA N-terminal domain (Fig. 2). The positions of amino acids 87 and 91 on *H. pylori* GyrA corresponded to part of the head dimer interface of the *E. coli* GyrA N-terminal domain. The homology model of the *H. pylori* GyrA C-terminal domain also resembled the structure of the *E. coli* GyrA C-terminal domain (Fig. 3).

Discussion

Alignment of the *H. pylori gyrA* nucleotide sequence with that of *E. coli* also revealed that amino acids 87 and 91 in *H. pylori* correspond to amino acids 83 and 87 in *E. coli*.[14,18,20,27–30] Point mutations of amino acids 83 and 87 are known hot spots for quinolone resistance in *E. coli*.[31–33] It is proposed that the head dimer interface binds a segment of DNA, performs a double-stranded cleavage, and then pulls the broken ends of the DNA apart.[34] On the other hand, quinolones bind to a specific site on DNA in the DNA-enzyme complex.[16] Quinolones do not prevent the cleavage of the DNA but they interfere with the strand passage and re-ligation by stabilizing an intermediate of the catalytic cycle.[35] The head dimer interface is known to bind both DNA and quinolones.[36] Taken together, a mutation on the head dimer interface would have either a lower affinity for quinolones or a higher affinity for DNA, and prevent quinolones from binding to the DNA–enzyme complex.

We previously demonstrated a high resistance rate (47.9%) to gatifloxacin after eradication failure in Japan, and a significant association between gatifloxacin resistance and *gyrA* mutations in *H. pylori*.[30] On the other hand, we also demonstrated that the minimum inhibitory concentration (MIC) of garenoxacin was fourfold lower and that of sitafloxacin was 16-fold lower than that of gatifloxacin against the *H. pylori* strains with *gyrA* mutations.[37] These results suggest that new generation quinolones, such as sitafloxacin and garenoxacin, may overcome the resistance of *H. pylori* with *gyrA* mutations. The mechanism by which new generation quinolones would be able to overcome the resistance is still unknown. New generation quinolones may be able to bind mutant GyrA and inhibit the function of DNA gyrase. It is reported that sitafloxacin has a stronger activity to interact with the so-called quinolone pocket in GyrB.[38] However, *gyrB* mutation has not been described as involved in the quinolone resistance of *H. pylori*.[28] This suggests that new generation quinolones may also be able to bind *H. pylori* GyrB stronger than other quinolones. Switching to these new generation quinolones may improve the efficacy of quinolone-based *H. pylori* eradication therapy.

The target of quinolones is not only DNA gyrase, but also topoisomerase IV, in several bacteria.[39–42] Genome sequencing has revealed that *H. pylori* lacks the topoisomerase IV *parC* and *parE* genes.[43,44] In addition, multidrug efflux pumps do not yet appear to mediate quinolone resistance,[45] which suggests that DNA gyrase in a unique target of quinolones in *H. pylori*. Therefore, it is important to investigate the structure of DNA gyrase in *H. pylori* in order to overcome the mechanism of quinolone resistance.

In conclusion, the structure of *H. pylori* GyrA resembles that of *E. coli* GyrA. The unique target of quinolones is supposed to be the head dimer interface of GyrA in *H. pylori*. Garenoxacin and sitafloxacin are likely to act differently to gatifloxacin against *H. pylori* GyrA.

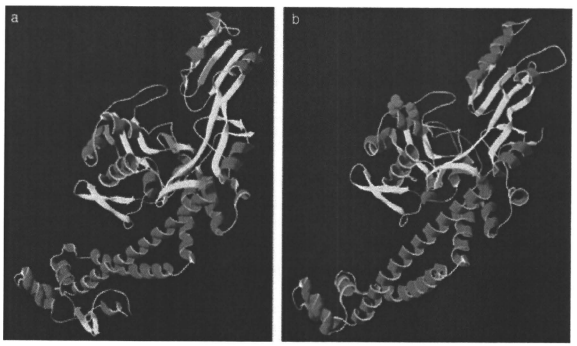

Figure 2 Comparison between *Helicobacter pylori* GyrA N-terminal domain and *Escherichia coli* GyrA N-terminal domain. (a) Crystal structure of *E. coli* GyrA N-terminal domain (Protein Data Bank code: 1ab4). (b) Homology model of *H. pylori* GyrA N-terminal domain generated by SWISS-MODEL. The mutations of amino acids 87 and 91 on *H. pylori* GyrA (green region) cause quinolone resistance.

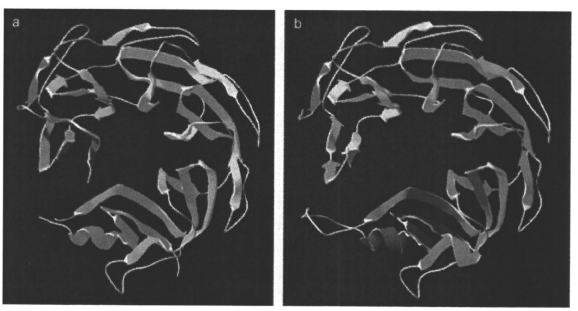

Figure 3 Comparison between *Helicobacter pylori* GyrA C-terminal domain and *Escherichia coli* GyrA C-terminal domain. (a) Structure of *E. coli* GyrA C-terminal domain (Protein Data Bank code: 1zi0B). (b) Homology model of *H. pylori* GyrA C-terminal domain generated by SWISS-MODEL.

References

1 Suzuki H, Hibi T, Marshall BJ. *Helicobacter pylori*: present status and future prospects in Japan. *J. Gastroenterol.* 2007; **42**: 1–15.
2 Amieva MR, El-Omar EM. Host-bacterial interactions in *Helicobacter pylori* infection. *Gastroenterology* 2008; **134**: 306–23.
3 Correa P, Houghton J. Carcinogenesis of *Helicobacter pylori*. *Gastroenterology* 2007; **133**: 659–72.
4 Shi R, Xu S, Zhang H *et al.* Prevalence and risk factors for *Helicobacter pylori* infection in Chinese populations. *Helicobacter* 2008; **13**: 157–65.
5 Suzuki H, Iwasaki E, Hibi T. *Helicobacter pylori* and gastric cancer. *Gastric Cancer* 2009; **12**: 79–87.
6 Kato M, Yamaoka Y, Kim JJ *et al.* Regional differences in metronidazole resistance and increasing clarithromycin resistance among *Helicobacter pylori* isolates from Japan. *Antimicrob. Agents Chemother.* 2000; **44**: 2214–16.
7 Osato MS, Reddy R, Graham DY. Metronidazole and clarithromycin resistance amongst *Helicobacter pylori* isolates from a large metropolitan hospital in the United States. *Int. J. Antimicrob. Agents* 1999; **12**: 341–7.
8 Nishizawa T, Suzuki H, Umezawa A *et al.* Rapid detection of point mutations conferring resistance to fluoroquinolone in gyrA of *Helicobacter pylori* by allele-specific PCR. *J. Clin. Microbiol.* 2007; **45**: 303–5.
9 Nishizawa T, Suzuki H, Nakagawa I, Iwasaki E, Masaoka T, Hibi T. Gatifloxacin-based triple therapy as a third-line regimen for *Helicobacter pylori* eradication. *J. Gastroenterol. Hepatol.* 2008; **23** (Suppl. 2): S167–70.
10 Suzuki S, Suzuki H, Nishizawa T *et al.* Past rifampicin dosing determines rifabutin resistance of *Helicobacter pylori*. *Digestion* 2009; **79**: 1–4.
11 Gisbert JP, Castro-Fernandez M, Bermejo F *et al.* Third-line rescue therapy with levofloxacin after two *H. pylori* treatment failures. *Am. J. Gastroenterol.* 2006; **101**: 243–7.
12 Cianci R, Montalto M, Pandolfi F, Gasbarrini GB, Cammarota G. Third-line rescue therapy for *Helicobacter pylori* infection. *World J. Gastroenterol.* 2006; **12**: 2313–9.
13 Nishizawa T, Suzuki H, Hibi T. Quinolone-based third-line therapy for *Helicobacter pylori* eradication. *J. Clin. Biochem. Nutr.* 2009; **44**: 119–24.
14 Sharara AI, Chaar HF, Aoun E, Abdul-Baki H, Araj GF, Kanj SS. Efficacy and safety of rabeprazole, amoxicillin, and gatifloxacin after treatment failure of initial *Helicobacter pylori* eradication. *Helicobacter* 2006; **11**: 231–6.
15 Tanaka M, Isogai E, Isogai H *et al.* Synergic effect of quinolone antibacterial agents and proton pump inhibitors on *Helicobacter pylori*. *J. Antimicrob. Chemother.* 2002; **49**: 1039–40.
16 Shen LL, Kohlbrenner WE, Weigl D, Baranowski J. Mechanism of quinolone inhibition of DNA gyrase. Appearance of unique

norfloxacin binding sites in enzyme-DNA complexes. *J. Biol. Chem.* 1989; **264**: 2973–8.
17 Reece RJ, Maxwell A. DNA gyrase: structure and function. *Crit. Rev. Biochem. Mol. Biol.* 1991; **26**: 335–75.
18 Wang G, Wilson TJ, Jiang Q, Taylor DE. Spontaneous mutations that confer antibiotic resistance in *Helicobacter pylori*. *Antimicrob. Agents Chemother.* 2001; **45**: 727–33.
19 Megraud F. Epidemiology and mechanism of antibiotic resistance in *Helicobacter pylori*. *Gastroenterology* 1998; **115**: 1278–82.
20 Moore RA, Beckthold B, Wong S, Kureishi A, Bryan LE. Nucleotide sequence of the gyrA gene and characterization of ciprofloxacin-resistant mutants of *Helicobacter pylori*. *Antimicrob. Agents Chemother.* 1995; **39**: 107–11.
21 Schwede T, Kopp J, Guex N, Peitsch MC. SWISS-MODEL: an automated protein homology-modeling server. *Nucleic Acids Res.* 2003; **31**: 3381–5.
22 Bordoli L, Kiefer F, Arnold K, Benkert P, Battey J, Schwede T. Protein structure homology modeling using SWISS-MODEL workspace. *Nat. Protoc.* 2009; **4**: 1–13.
23 Guex N, Peitsch MC. SWISS-MODEL and the Swiss-PdbViewer: an environment for comparative protein modelling. *Electrophoresis* 1997; **18**: 2714–23.
24 Arnold K, Bordoli L, Kopp J, Schwede T. The SWISS-MODEL workspace: a web-based environment for protein structure homology modelling. *Bioinformatics* 2006; **22**: 195–201.
25 Morais Cabral JH, Jackson AP, Smith CV, Shikotra N, Maxwell A, Liddington RC. Crystal structure of the breakage-reunion domain of DNA gyrase. *Nature* 1997; **388**: 903–6.
26 Ruthenburg AJ, Graybosch DM, Huetsch JC, Verdine GL. A superhelical spiral in the Escherichia coli DNA gyrase A C-terminal domain imparts unidirectional supercoiling bias. *J. Biol. Chem.* 2005; **280**: 26177–84.
27 Swanberg SL, Wang JC. Cloning and sequencing of the Escherichia coli gyrA gene coding for the A subunit of DNA gyrase. *J. Mol. Biol.* 1987; **197**: 729–36.
28 Tankovic J, Lascols C, Sculo Q, Petit JC, Soussy CJ. Single and double mutations in gyrA but not in gyrB are associated with low- and high-level fluoroquinolone resistance in *Helicobacter pylori*. *Antimicrob. Agents Chemother.* 2003; **47**: 3942–4.
29 Glocker E, Kist M. Rapid detection of point mutations in the gyrA gene of *Helicobacter pylori* conferring resistance to ciprofloxacin by a fluorescence resonance energy transfer-based real-time PCR approach. *J. Clin. Microbiol.* 2004; **42**: 2241–6.
30 Nishizawa T, Suzuki H, Kurabayashi K *et al.* Gatifloxacin resistance and mutations in gyra after unsuccessful Helicobacter pylori eradication in Japan. *Antimicrob. Agents Chemother.* 2006; **50**: 1538–40.
31 Drlica K, Zhao X. DNA gyrase, topoisomerase IV, and the 4-quinolones. *Microbiol. Mol. Biol. Rev.* 1997; **61**: 377–92.
32 Heisig P, Kratz B, Halle E *et al.* Identification of DNA gyrase A mutations in ciprofloxacin-resistant isolates of Salmonella typhimurium from men and cattle in Germany. *Microb. Drug Resist.* 1995; **1**: 211–18.
33 Willmott CJ, Maxwell A. A single point mutation in the DNA gyrase A protein greatly reduces binding of fluoroquinolones to the gyrase-DNA complex. *Antimicrob. Agents Chemother.* 1993; **37**: 126–7.
34 Williams NL, Maxwell A. Locking the DNA gate of DNA gyrase: investigating the effects on DNA cleavage and ATP hydrolysis. *Biochemistry* 1999; **38**: 14157–64.
35 Siegmund K, Maheshwary S, Narayanan S *et al.* Molecular details of quinolone-DNA interactions: solution structure of an unusually stable DNA duplex with covalently linked nalidixic acid residues and non-covalent complexes derived from it. *Nuclei. Acids Res.* 2005; **33**: 4838–48.
36 Barnard FM, Maxwell A. Interaction between DNA gyrase and quinolones: effects of alanine mutations at GyrA subunit residues Ser(83) and Asp(87). *Antimicrob. Agents Chemother.* 2001; **45**: 1994–2000.
37 Suzuki H, Nishizawa T, Muraoka H, Hibi T. Sitafloxacin and garenoxacin may overcome the antibiotic resistance of Helicobacter pylori with gyrA mutation. *Antimicrob. Agents Chemother.* 2009; **53**: 1720–1.
38 Akasaka T, Kurosaka S, Uchida Y, Tanaka M, Sato K, Hayakawa I. Antibacterial activities and inhibitory effects of sitafloxacin (DU-6859a) and its optical isomers against type II topoisomerases. *Antimicrob. Agents Chemother.* 1998; **42**: 1284–7.
39 Yoshida H, Bogaki M, Nakamura M, Yamanaka LM, Nakamura S. Quinolone resistance-determining region in the DNA gyrase gyrB gene of Escherichia coli. *Antimicrob. Agents Chemother.* 1991; **35**: 1647–50.
40 Heddle J, Maxwell A. Quinolone-binding pocket of DNA gyrase: role of GyrB. *Antimicrob. Agents Chemother.* 2002; **46**: 1805–15.
41 Ferrero L, Cameron B, Manse B *et al.* Cloning and primary structure of Staphylococcus aureus DNA topoisomerase IV: a primary target of fluoroquinolones. *Mol. Microbiol.* 1994; **13**: 641–53.
42 Khodursky AB, Cozzarelli NR. The mechanism of inhibition of topoisomerase IV by quinolone antibacterials. *J. Biol. Chem.* 1998; **273**: 27668–77.
43 Alm RA, Ling LS, Moir DT *et al.* Genomic-sequence comparison of two unrelated isolates of the human gastric pathogen *Helicobacter pylori*. *Nature* 1999; **397**: 176–80.
44 Tomb JF, White O, Kerlavage AR *et al.* The complete genome sequence of the gastric pathogen Helicobacter pylori. *Nature* 1997; **388**: 539–47.
45 Bina JE, Alm RA, Uria-Nickelsen M, Thomas SR, Trust TJ, Hancock RE. Helicobacter pylori uptake and efflux: basis for intrinsic susceptibility to antibiotics in vitro. *Antimicrob. Agents Chemother.* 2000; **44**: 248–54.

neurogastroenterology & motility

Neurogastroenterol Motil (2010) **22**, 595–599 doi: 10.1111/j.1365-2982.2010.01486.x

VIEWPOINT

Acotiamide (Z-338) as a possible candidate for the treatment of functional dyspepsia

H. SUZUKI & T. HIBI

Division of Gastroenterology and Hepatology, Department of Internal Medicine, Keio University School of Medicine, Tokyo, Japan

Abstract

Acotiamide hydrochloride is a novel upper gastrointestinal (GI) motility modulator and stress regulator currently being developed for the treatment of functional dyspepsia (FD). The mechanism underlying the enhancement of GI motility by this agent has been proposed to be based on its muscarinic antagonism and inhibitory effects on acetylcholinesterase activity. Pathophysiological studies showed that acotiamide significantly improved both delayed gastric emptying and feeding inhibition in restraint stress-induced model, but did not affect both normal gastric emptying and feeding in intact animals, indicating that acotiamide exerted effects only on the impaired gastric emptying and feeding behavior. According to the clinical pilot study in Europe, acotiamide, at the dose of 100 mg t.i.d., showed to improve the symptoms and quality of life of patients with FD, indicating the need for larger scale symptomatic studies on the efficacy of acotiamide in patients with FD. The recent phase II studies conducted in Japan presented in this issue of the journal also confirmed that acotiamide, at the optimal dose of 100 mg, has potential therapeutic efficacy, especially for meal-related FD symptoms. Although a phase III study is on going, acotiamide is now expected as a novel treatment option for FD.

Keywords *acetylcholine, acetylcholinesterase, muscarinic, prokinetics, Rome III, symptom.*

Address for Correspondence
Hidekazu Suzuki, MD, PhD, FACG, Division of Gastroenterology and Hepatology, Department of Internal Medicine, Keio University School of Medicine, 35 Shinanomachi, Shinjuku-ku, Tokyo 160-8582, Japan.
Tel: +81 3 5363 3914; fax: +81 3 5363 3967;
e-mail: hsuzuki@sc.itc.keio.ac.jp
Received: 3 February 2010
Accepted for publication: 7 February 2010

INTRODUCTION

Functional dyspepsia (FD) is a clinical syndrome characterized by symptoms originating from the region of the stomach and duodenum, in the absence of explainable organic disease.[1,2] According to the Rome III criteria, the major symptoms of FD consist of bothersome postprandial fullness, early satiety, epigastralgia, and epigastric burning.[1,2] The symptom pattern and the underlying pathophysiology of FD are heterogeneous. Visceral hypersensitivity in response to distension,[3] impaired meal accommodation,[4] and delayed gastric emptying[5,6] have frequently been demonstrated in patients with FD. Furthermore, the involvement of several other mechanisms has also been suggested, including duodenal hypersensitivity to the luminal contents, small bowel dysmotility, *Helicobacter pylori* infection,[7,8] psychological disturbances, and central nervous system (CNS) disorders.[9]

There are several therapeutic options, including herbal medicines,[10] for patients with FD,[2] however, proven and satisfactory treatment strategies are still limited. As one of the possible strategies, treatment based on the underlying pathophysiological disorders mentioned above might seem to be a logical option. Unlike its analogs, the recently introduced acotiamide hydrochloride trihydrate (Z-338), [*N*-{*N*9,*N*9-diisopropylaminoethyl}-[2-(2-hydroxy-4,5-dimethoxy-benzoylamino)-1,3-thiazole-4-yl] carboxyamide monohydrochloride trihydrate] has little affinity for serotonin 5-HT_2, 5-HT_3 and 5-HT_4 receptors, and weak affinity for dopamine D2 receptors, whereas having a strong affinity for muscarinic M_1/M_2 receptors. Acotiamide exerts gastroprokinetic activity, partly by enhancement of acetylcholine (ACh) release via its antagonistic actions on the M_1, M_2 muscarinic

receptors, and partly by inhibiting acetylcholinesterase (AChE) activity. In addition, acotiamide may also act directly on the gut and indirectly on the CNS through the brain gut axis. Acotiamide is now expected as a novel treatment option for FD, especially the meal-related syndrome.

PHARMACOLOGICAL DATA OF ACOTIAMIDE

Although acotiamide enhances the gastrointestinal (GI) motility in conscious dogs, unlike conventional prokinetic agents such as itopride[11,12] or mosapride,[13] it has only weak affinity for the dopamine D_2 receptor and no affinity for the serotonin 5-HT_2, 5-HT_3, and 5-HT_4 receptors. It has been suggested that the drug enhances GI motility via facilitation of acetylcholine release from the enteric cholinergic nerve terminals.[14,15]

According to a basic study,[15] acotiamide inhibits the activity of AChE derived from human erythrocyte membranes and produces contraction of antrum preparations from the guinea pig stomach *in vitro*, and enhances the GI motility in conscious dogs and gastric emptying in rats and dogs *in vivo*. Among the muscarinic M_1, M_2, and M_3 receptors present in the neurons and/or smooth muscle cells of the GI tract, acotiamide acts as an antagonist on the M_1 and M_2 receptors.[15] These muscarinic receptors appear to be located on the cholinergic nerve terminals and to operate as autoreceptors. The release of ACh from cholinergic nerves is modulated by a negative feedback mechanism that is triggered by the stimulation of presynaptic muscarinic receptors. In the enteric nervous system, the release of ACh from the guinea pig myenteric and submucosal plexus neurons is inhibited by the presynaptic M_1 receptor[16,17] and M_2 receptor in the rat antral mucosal or submucosal neurons.[18] Acotiamide facilitates ACh release from the cholinergic nerve terminals by blocking muscarinic M_1 and M_2 autoreceptors which regulate the release of ACh.[15,19] In *Xenopus* oocytes expressing M_1 and M_2 muscarinic receptors, acotiamide did not produce any response, but inhibited ACh-induced outward currents, indicating that the drug acts as an antagonist on the M_1 and M_2 muscarinic receptors.[15]

According to a report by Ogishima *et al.*,[15] contractions of strips of the guinea pig stomach were sensitive to tetrodotoxin and atropine, and were enhanced by acotimide, probably due to the facilitation of ACh release by the drug. They also showed that acotiamide enhanced the electrically stimulated outflow of tritium as a measure of ^3H ACh release from antral strips.[20]

In the guinea pig ileum, scopolamine has been shown to greatly facilitate the stimulated release of ACh in the presence of a cholinesterase inhibitor.[21] Thus, ACh release is clearly enhanced by inhibition of muscarinic autoreceptors by muscarinic antagonists when the cholinesterase activity is inhibited. The facilitation of ACh release in the presence of an M_1 receptor antagonist (pirenzepine) or M_2 receptor antagonist[15] could be attributed to blockade of the presynaptic M_1 and M_2 autoreceptors that are activated by ACh released from the nerve terminals. These findings suggest that acotiamide apparently does not increase ACh release simply by inhibiting acetylcholinesterase.

IN VIVO STUDIES

In an animal model, acotiamide reversed stress-induced delayed gastric emptying and feeding inhibition through inhibition of the expression of stress-induced genes in the hypothalamus and medulla oblongata.[22] Although the delayed gastric emptying was reversed by acotiamide in several animal models, normal or non-dysfunctional gastric emptying was unaffected by acotiamide, suggesting that acotiamide may alter the regulation of stress responses, to specifically improve the symptoms of FD caused or aggravated by stress.

The hypothalamic paraventricular nucleus (PVN) is a major site of the production and release of corticotropin-releasing factor (CRF). Released CRF activates the hypothalamic–pituitary–adrenal (HPA) axis, and also affects motility and sensitivity of the gut.[23] DNA microarray analysis of the hypothalamus and medulla oblongata in rats[22] showed that acotiamide exerted an impact on the expression of genes related to the expression of neuromedin U (NmU), known as a stress-related neuropeptide[24] that suppresses food intake and induces delayed gastric emptying,[25,26] and to GABA/glutamate, which are major excitatory and inhibitory neurotransmitters within the CNS,[27] and mediates restraint stress-induced delayed gastric emptying.[28,29] Following administration of acotiamide, although the expression of NmU mRNA in the hypothalamus and the increase of its expression induced by restraint stress were suppressed, the delayed gastric emptying induced by administration of exogenous NmU or CRF was not reversed,[22] suggesting that while acotiamide may have a partial effect on the stress response, it does not reduce stress.

Taken together with the results of these animal studies, it is concluded that acotiamide is most probably to reverse delayed gastric emptying, feeding inhibition, and altered expression of stress-related genes in the brain stem that are induced by restrain stress.[22]

CLINICAL STUDIES OF ACOTIAMIDE

Previously, a double-blind, parallel-group trial of 12 weeks duration (after a 2 weeks PPI run-in and 2 weeks washout) randomized patients with FD (based on Rome II criteria) to placebo, 300 mg acotiamide, 600 mg acotiamide and 900 mg acotiamide, all three times daily.[30] According to this study, therapeutic gain was highest in the first month. In terms of the influence of PPI run-in, pH monitoring and nutrient tolerance on efficacy outcomes of acotiamide, the yield of a PPI run-in was low, and a nutrient challenge test, but not pH monitoring, would predict responsiveness of acotiamide.[31] Among dose ranges, acotiamide 300 mg significantly improved postprandial epigastric pain and nausea at 4 weeks, and significantly improving 3 of 5 quality of life Nepean Dyspepsia Index scales. According to their report, adverse events were minor and similar across all arms.[30]

Then, Tack *et al.* conducted a randomized, double-blind, placebo-controlled, parallel-group study on 71 patients from eight European centres (62 evaluable) with lower doses of acotiamide (50, 100, and 300 mg). In their pilot study, although there was no effect of the drug on gastric emptying as evaluated by the ^{13}C octanoic acid breath test and sensitivity to distension based on gastric barostat studies, acotiamide exhibited the potential to improve FD symptoms as assessed by the overall symptom scores based on the severity and frequency of nine dyspeptic symptoms, and also the quality of life (QOL) as assessed by the SF-36 questionnaire. In that study, 300 mg was better than placebo for meal accommodation and 100 mg acotiamide was better than placebo at week 2 for upper abdominal bloating and the overall symptom score, and at week 3 for bloating and heartburn.[32] Moreover, 100 mg acotiamide was also better than placebo for the QOL (physical function). This pilot study concluded that at the dose of 100 mg t.i.d., acotiamide showed the potential to improve the symptoms and QOL of patients with FD, indicating the need for larger scale symptomatic studies on the efficacy of acotiamide in patients with FD.

Although the optimal endpoint to be used in FD clinical trials has not yet been established, 'the subjects' global assessment of overall treatment efficacy (OTE)', recommended for use as the primary endpoint by the Rome group, evaluates improvement and worsening by means of a 7-point symmetrical Likert scale, it overcomes some of the limitations of a binary endpoint. Matsueda *et al.* also chose the improvement rate of 'the subjects' global assessment of OTE' at the final evaluation as the primary endpoint in their study conducted to determine the dose-dependent therapeutic efficacy of acotiamide in patients with FD. They reported the results of two randomized, double blind, placebo controlled, parallel-group, comparative studies of acotiamide in Japanese FD patients in the present issue of Neurogastroenterology and Motility.[33] Both studies consisted of a baseline period of 8 days, followed by a randomized controlled treatment period of 28 days, during which the patients were allocated to placebo or different doses of acotiamide (50, 100 or 300 mg t.i.d.). In their study 1, the OTE was 41.7% in the placebo group, 51.5% in the 100-mg cohort, and 49.5% in the 300-mg cohort, while those in their study 2, the values were 49.1% in the placebo group, 48.7% in the 50-mg cohort, 58.3% in the 100-mg cohort, and 56.9% in the 300-mg cohort, suggesting that the improvement rates were approximately 10% higher in the 100-mg acotiamide cohorts than in the placebo groups, with good reproducibility. The elimination rate of postprandial fullness in the 100-mg acotiamide cohort was significantly higher than that in the placebo group. In the absence of effective treatment options for FD, the 10% gain over placebo may be considered as clinically and scientifically significant. The phase II studies conducted by the same group confirmed that acotiamide, at the optimal dose of 100 mg, has potential therapeutic efficacy, especially for meal-related FD symptoms. At present the results of phase III studies on the efficacy of 100 mg acotiamide in FD patients are awaited.

SUMMARY

Functional dyspepsia is a highly prevalent condition with few efficacious treatments. Although GI prokinetics have long been considered the therapeutic options of choice for the treatment of FD, on the basis of the assumption that delayed gastric emptying or poorly coordinated antro-pyloro-duodenal coordination was present in a majority of these patients, as there are poor correlation between delayed emptying and symptoms and the frequent co-existence of other sensorimotor disorders, the efficacy of prokinetics is usually limited. Acotiamide is a novel class of prokinetic drugs, which enhance acetylcholine release, and would be efficious for the FD therapy both by central and by peripheral way. As was shown in the results of recent phase II trials, acotiamide has been shown to have a symptomatic benefit for the treatment of FD, especially for meal-related syndrome, without major adverse effects. As generally known, management of patients with functional GI disorders has become more difficult because several

candidate drugs were associated with significant adverse events leading to the withdrawal of medication such as cisapride[34] and tegaserod.[35] For this reason, we need to be very careful for its safety and dose selection, based on the further results of well-organized clinical trials.

REFERENCES

1 Tack J, Talley NJ, Camilleri M *et al.* Functional gastroduodenal disorders. *Gastroenterology* 2006; **130**: 1466–79.
2 Suzuki H, Nishizawa T, Hibi T. Therapeutic strategies for functional dyspepsia and the introduction of the Rome III classification. *J Gastroenterol* 2006; **41**: 513–23.
3 Tack J, Caenepeel P, Fischler B, Piessevaux H, Janssens J. Symptoms associated with hypersensitivity to gastric distention in functional dyspepsia. *Gastroenterology* 2001; **121**: 526–35.
4 Tack J, Piessevaux H, Coulie B, Caenepeel P, Janssens J. Role of impaired gastric accommodation to a meal in functional dyspepsia. *Gastroenterology* 1998; **115**: 1346–52.
5 Sarnelli G, Caenepeel P, Geypens B, Janssens J, Tack J. Symptoms associated with impaired gastric emptying of solids and liquids in functional dyspepsia. *Am J Gastroenterol* 2003; **98**: 783–8.
6 Stanghellini V, Tosetti C, Paternic inverted question marko A *et al.* Risk indicators of delayed gastric emptying of solids in patients with functional dyspepsia. *Gastroenterology* 1996; **110**: 1036–42.
7 Suzuki H, Masaoka T, Sakai G, Ishii H, Hibi T. Improvement of gastrointestinal quality of life scores in cases of *Helicobacter pylori*-positive functional dyspepsia after successful eradication therapy. *J Gastroenterol Hepatol* 2005; **20**: 1652–60.
8 Suzuki H, Hibi T, Marshall BJ. *Helicobacter pylori*: present status and future prospects in Japan. *J Gastroenterol* 2007; **42**: 1–15.
9 Wilmer A, Van Cutsem E, Andrioli A, Tack J, Coremans G, Janssens J. Ambulatory gastrojejunal manometry in severe motility-like dyspepsia: lack of correlation between dysmotility, symptoms, and gastric emptying. *Gut* 1998; **42**: 235–42.
10 Suzuki H, Inadomi JM, Hibi T. Japanese herbal medicine in functional gastrointestinal disorders. *Neurogastroenterol Motil* 2009; **21**: 688–96.
11 Iwanaga Y, Kimura T, Miyashita N *et al.* Characterization of acetylcholinesterase-inhibition by itopride. *Jpn J Pharmacol* 1994; **66**: 317–22.
12 Iwanaga Y, Miyashita N, Morikawa K, Mizumoto A, Kondo Y, Itoh Z. A novel water-soluble dopamine-2 antagonist with anticholinesterase activity in gastrointestinal motor activity. Comparison with domperidone and neostigmine. *Gastroenterology* 1990; **99**: 401–8.
13 Yoshida N, Omoya H, Kato S, Ito T. Pharmacological effects of the new gastroprokinetic agent mosapride citrate and its metabolites in experimental animals. *Arzneimittelforschung* 1993; **43**: 1078–83.
14 Nakajima T, Nawata H, Ito Y. Z-338, a newly synthetized carboxyamide derivative, stimulates gastric motility through enhancing the excitatory neurotransmission. *J Smooth Muscle Res* 2000; **36**: 69–81.
15 Ogishima M, Kaibara M, Ueki S, Kurimoto T, Taniyama K. Z-338 facilitates acetylcholine release from enteric neurons due to blockade of muscarinic autoreceptors in guinea pig stomach. *J Pharmacol Exp Ther* 2000; **294**: 33–7.
16 Kawashima K, Fujimoto K, Suzuki T, Oohata H. Direct determination of acetylcholine release by radioimmunoassay and presence of presynaptic M1 muscarinic receptors in guinea pig ileum. *J Pharmacol Exp Ther* 1988; **244**: 1036–9.
17 Schworer H, Kilbinger H. Enhancement of guinea-pig intestinal peristalsis by blockade of muscarinic M1-receptors. *Br J Pharmacol* 1988; **93**: 715–20.
18 Ren J, Harty RF. Presynaptic muscarinic receptors modulate acetylcholine release from rat antral mucosal/submucosal nerves. *Dig Dis Sci* 1994; **39**: 1099–106.
19 Doi Y, Murasaki O, Kaibara M *et al.* Characterization of functional effects of Z-338, a novel gastroprokinetic agent, on the muscarinic M1, M2, and M3 receptors expressed in *Xenopus* oocytes. *Eur J Pharmacol* 2004; **505**: 31–5.
20 Kusunoki M, Taniyama K, Tanaka C. Dopamine regulation of [3H]acetylcholine release from guinea-pig stomach. *J Pharmacol Exp Ther* 1985; **234**: 713–9.
21 Kilbinger H, Wessler I. Inhibition by acetylcholine of the stimulation-evoked release of [3H]acetylcholine from the guinea-pig myenteric plexus. *Neuroscience* 1980; **5**: 1331–40.
22 Seto K, Sasaki T, Katsunuma K, Kobayashi N, Tanaka K, Tack J. Acotiamide hydrochloride (Z-338), a novel prokinetic agent, restores delayed gastric emptying and feeding inhibition induced by restraint stress in rats. *Neurogastroenterol Motil* 2008; **20**: 1051–9.
23 Monnikes H, Tebbe JJ, Hildebrandt M *et al.* Role of stress in functional gastrointestinal disorders. Evidence for stress-induced alterations in gastrointestinal motility and sensitivity. *Dig Dis* 2001; **19**: 201–11.
24 Hanada R, Nakazato M, Murakami N *et al.* A role for neuromedin U in stress response. *Biochem Biophys Res Commun* 2001; **289**: 225–8.
25 Howard AD, Wang R, Pong SS *et al.* Identification of receptors for neuromedin U and its role in feeding. *Nature* 2000; **406**: 70–4.
26 Mondal MS, Date Y, Murakami N *et al.* Neuromedin U acts in the central nervous system to inhibit gastric acid secretion via CRH system. *Am J Physiol Gastrointest Liver Physiol* 2003; **284**: G963–9.
27 Zhang X, Fogel R. Involvement of glutamate in gastrointestinal vagovagal reflexes initiated by gastrointestinal distention in the rat. *Auton Neurosci* 2003; **103**: 19–37.
28 Sivarao DV, Krowicki ZK, Hornby PJ. Role of GABAA receptors in rat hindbrain nuclei controlling gastric motor function. *Neurogastroenterol Motil* 1998; **10**: 305–13.
29 Iwa M, Nakade Y, Pappas TN, Takahashi T. Electroacupuncture improves restraint stress-induced delay of gastric emptying via central glutaminergic pathways in conscious rats. *Neurosci Lett* 2006; **399**: 6–10.
30 Talley NJ, Tack JF, Kowalski DL, Borton MA, Barve A. A novel acetylcholine esterase inhibitor acotiamide hydrochloride (YM443) in functional

dyspepsia: efficacy in a randomized, double-blinded, placebo-controlled dose ranging trial. *Gastroenterology* 2008; **134**: A157–8.

31 Tack JF, Talley NJ, Kowalski DL, Borton MA, Barve A. Influence of PPI run-in, pH monitoring and nutrient tolerance on efficacy outcomes of acotiamide hydrochloride (YM443), a novel acetylcholine esterase inhibitor, in functional dyspepsia. *Gastroenterology* 2008; **134**: A143.

32 Tack J, Masclee A, Heading R *et al.* A dose-ranging, placebo-controlled, pilot trial of acotiamide in patients with functional dyspepsia. *Neurogastroenterol Motil* 2009; **21**: 272–80.

33 Matsueda K, Hongo M, Tack J, Aoki H, Saito Y, Kato H. Clinical trial: dose-dependent therapeutic efficacy of acotiamide hydrochloride (Z-338) in patients with functional dyspepsia – 100 mg t.i.d. is an optimal dosage. *Neurogastroenterol Motil* 2010; in press.

34 Glessner MR, Heller DA. Changes in related drug class utilization after market withdrawal of cisapride. *Am J Manag Care* 2002; **8**: 243–50.

35 Pasricha PJ. Desperately seeking serotonin. A commentary on the withdrawal of tegaserod and the state of drug development for functional and motility disorders. *Gastroenterology* 2007; **132**: 2287–90.

Dig Dis Sci (2010) 55:3339–3348
DOI 10.1007/s10620-010-1167-8

ORIGINAL ARTICLE

Acid Suppression by Proton Pump Inhibitors Enhances Aquaporin-4 and KCNQ1 Expression in Gastric Fundic Parietal Cells in Mouse

Juntaro Matsuzaki · Hidekazu Suzuki · Yuriko Minegishi · Etsuko Sugai · Hitoshi Tsugawa · Masato Yasui · Toshifumi Hibi

Received: 12 September 2009 / Accepted: 11 February 2010 / Published online: 1 May 2010

Abstract
Background The widespread use of proton pump inhibitors (PPIs) is known to cause sporadic gastric fundic gland polyps (FGPs). Altered expression and localization of the water or ion transport proteins might contribute to the excess fluid secretion into the cystic lumen for the development of FGPs.
Aims We investigated the alteration of the murine gastric fundic mucosa after PPI treatment, and examined the expression of water channel aquaporin-4 (AQP4) and potassium channel KCNQ1, which are expressed only in the parietal cells in the gastric mucosa.
Methods Male 5-week-old C57BL/6J mice were administered lansoprazole (LPZ) by subcutaneous injection for 8 weeks. The expression of AQP4 and KCNQ1 were investigated by Western blotting, quantitative RT-PCR, and immunohistochemistry. The expression of mucin-6 (Muc6), pepsinogen, and sonic hedgehog (Shh) were also investigated as mucosal cell lineage markers.
Results Gastric mucosal hyperplasia with multiple cystic dilatations, exhibiting similar histological findings to the FGPs, was observed in the LPZ-treated mice. An increase in the number of AQP4-positive parietal cells and KCNQ1-positive parietal cells was observed. The extension of the distribution of AQP4-positive cells toward the surface of the fundic glands was also observed. The expression levels of AQP4 mRNA and protein were significantly enhanced. The expression of KCNQ1 mRNA was correlated with that of AQP4 mRNA in the LPZ-treated mice. Mucous neck-to-zymogenic cell lineage differentiation was delayed in association with decreased expression of Shh in the LPZ-treated mice.
Conclusions PPI administration increased the number of parietal cells with enhanced expression of AQP4 and KCNQ1.

Keywords Proton pump inhibitors · Aquaporins · Potassium channels · Fundic gland polyps

Introduction

Proton pump inhibitors (PPIs) strongly inhibit the function of H^+/K^+-ATPase in gastric parietal cells, causing profound suppression of acid secretion. The use of PPIs has become widespread for the treatment of peptic ulcer disease and gastroesophageal reflux disease [1]. Such widespread use of PPIs has recently come to be known to be associated with the formation of gastric sporadic fundic gland polyps (FGPs), particularly in patients with *Helicobacter pylori*-free stomachs [2, 3]. FGPs are the most common gastric polyps [4]. A recent study showed that the prevalence of gastric polyps in the esophagogastroduodenoscopy population was 6.4% in the USA, and 77% of these lesions were FGPs [5]. FGPs are defined as cystic dilatations of the oxyntic glands lined by variably flattened parietal and chief cells with or without foveolar

Electronic supplementary material The online version of this article (doi:10.1007/s10620-010-1167-8) contains supplementary material, which is available to authorized users.

J. Matsuzaki · H. Suzuki (✉) · Y. Minegishi · E. Sugai · H. Tsugawa · T. Hibi
Division of Gastroenterology and Hepatology, Department of Internal Medicine, Keio University School of Medicine, 35 Shinanomachi, Shinjuku-ku, Tokyo 160-8582, Japan
e-mail: hsuzuki@sc.itc.keio.ac.jp

M. Yasui
Department of Pharmacology, Keio University School of Medicine, 35 Shinanomachi, Shinjuku-ku, Tokyo 160-8582, Japan

cells [6–8]. Although the mechanism of the development of the cystic dilatations in the fundic glands is not fully understood, increased fluid secretion into the cystic lumen is believed to play an important role.

The aquaporins (AQPs) are a family of small integral plasma membrane proteins that primarily transport water across the plasma membrane driven by osmotic gradients [9–11]. Although aquaporin-4 (AQP4) is expressed predominantly on the basolateral membrane of the parietal cells, the function of AQP4 in the stomach still remains unknown. In AQP4 knockout mice, a tendency towards decrease in fluid secretion in the fundic glands has been observed [12]. A recent study suggested that the expression of AQP4 played key roles in the proliferation of gastric epithelial cells and tumor biology [13].

KCNQ1 and its subunit KCNE2 are also expressed predominantly in the parietal cells [14], and both proteins unite to form a voltage-gated potassium channel [15–17]. KCNQ1 channel blockers inhibit acid secretion [14, 16, 17], and both KCNQ1-deficient and KCNE2-deficient mice exhibit loss of acid secretion [18–21], suggesting an essential role of KCNQ1 in acid secretion.

Since PPIs exert histamine-, gastrin- and acetylcholine-independent inhibition of acid secretion, chronic PPI usage is known to induce hypergastrinemia [22, 23]. In gastrin knockout mice, in which the parietal cells are reduced in number and the mRNA expression of the H^+/K^+-ATPase β subunit is reduced [24], the expressions of AQP4 and KCNQ1 were decreased and was reversed by gastrin supplementation [25]. Therefore, we hypothesized that the expression of AQP4 and KCNQ1 may be altered by PPI administration, and that the altered expression and localization of these transport proteins might contribute to the development of FGPs associated with PPI administration.

High-dose and long-term PPI treatment has been reported to cause various morphological changes in the gastric fundic glands of rats, such as increase in the number of small mucous neck cells, of cystic degenerative cells with amorphous eosinophilic contents and of acinar-cell-like cells with red granules, and decrease in the number of chief cells [26]. In addition, we previously reported that gastric hypochlorhydria caused impaired mucous neck-to-zymogenic cell lineage differentiation in the fundic glands of *H. pylori*-colonized Mongolian gerbils [27, 28] and histamine H_2 receptor (H_2R)-null mice, with suppressed sonic hedgehog (Shh) expression [22, 29, 30]. Shh is believed to regulate epithelial cell differentiation in the adult stomach [28, 31, 32]. All of these results of previous studies prompted us to examine whether gastric acid suppression by PPI administration might influence Shh expression and the homeostasis of the gastric mucosa.

Interestingly, AQP4-positive parietal cells are localized principally in the lower part of the gastric fundic glands [33]. In addition, KCNQ1 expression is stronger in the lower parietal cells than in the upper parietal cells, although KCNQ1-positive parietal cells are widely observed in the isthmus and neck region of the fundic glands [17, 34]. These findings suggest that the functions of parietal cells may differ depending on their vertical localization in the gastric fundic glands, and that AQP4 and KCNQ1 could be useful markers to investigate impaired parietal cell differentiation.

In the present study, we showed the disturbance of parietal cell differentiation and mucous neck-to-zymogenic cell lineage differentiation with enhanced expression of AQP4 and KCNQ1 in the parietal cells.

Methods

Animals

Male 5-week-old C57BL/6J mice were purchased from Sankyo Labo (Tokyo, Japan). All the mice were used for the study after acclimatization for 1 week. The proton pump inhibitor, lansoprazole (LPZ), was gifted from Takeda Pharm. Co., Ltd. (Tokyo, Japan). The mice in the LPZ-treated group ($n = 10$) were administered LPZ at the dose of 30 mg/kg, 1 x/day, by subcutaneous injection for 8 weeks. The mice in the control group ($n = 11$) were administered vehicle (0.5% CMC solution) by subcutaneous injection for 8 weeks. The experimental mice were killed after 24 h of food deprivation, although access to water was not restricted, and the stomachs were resected and blood samples obtained. The gastric surface pH was measured with a pH meter using a flat probe (D-51, Horiba Ltd, Kyoto, Japan). The blood samples were withdrawn from the orbital plexus of the experimental mice with a capillary tube. The samples were centrifuged at 6,000 $\times$ *g* for 15 min to separate the serum. Gastrin concentrations were determined by radioimmunoassay using human gastrin-17 as the standard (Mitsubishi Chemical Medience, Tokyo, Japan). All the experiments and procedures in the present study were approved by the Keio University Animal Research Committee.

Histology, Immunohistochemistry, and Immunofluorescence

The lesser curvature of the stomach tissue specimens from the experimental mice were fixed in 10% neutralized buffered formalin, embedded in paraffin, placed on poly-L-lysine-pretreated slides, and then stained with hematoxylin and eosin (H&E) for histological examination.

The antibodies used for the immunohistochemistry are listed below: rat monoclonal anti-Ki67 antibody (TEC-3,

1:25, Dako Japan, Tokyo, Japan), rabbit polyclonal anti-AQP4 antibody (AB3068, 1:100, Chemicon, CA, USA), goat polyclonal anti-KCNQ1 antibody (sc-10646, 1:100, Santa Cruz, CA, USA), mouse monoclonal anti-H^+/K^+-ATPase α subunit antibody (clone 1H9, 1:300, Research Diagnostics, NJ, USA), rabbit anti-mouse pepsinogen C antibody (mPep; a kind gift from Dr. Yasushi Fukushima), and mouse monoclonal anti-Muc6 antibody (HIK1083, 1:30, Kanto Chemical, Tokyo, Japan).

For immunohistochemistry, after deparaffinization and rehydration, the antigens were retrieved by heating in citrate buffer (10 mM, pH 6.0) for anti-mouse pepsinogen C antibody (121°C, 15 min), anti-AQP4 antibody (105°C, 10 min), and anti-KCNQ1 antibody (105°C, 10 min). For anti-Ki67 antibody, anti-H^+/K^+-ATPase and anti-Muc6 antibodies, the sections were digested with proteinase K solution (Dako Japan, Tokyo, Japan) for 4 min at room temperature. After the antigen retrieval, endogenous non-specific peroxidases were quenched with 0.3% hydrogen peroxide. Nonspecific binding was blocked by a blocking reagent (Protein Block, Dako Japan). For H^+/K^+-ATPase and Muc6 staining, the Nichirei Histofine Mouse Staining Kit (Nichirei, Tokyo, Japan) was used in order to eliminate endogenous mouse Ig cross-staining. Sections were incubated overnight with each of the primary antibodies at 4°C. After rinsing in TBS-T, the slides were incubated with HRP-labeled anti-rat IgG, anti-goat IgG, anti-rabbit IgG, or anti-mouse IgG (HISTOFINE, Simple stain MAX-PO (Rat/Goat/Rabbit/Mouse; Nichirei)) for 30 min at room temperature. Thereafter, staining was developed with 3,3′-diaminobenzidine tetrahydrochloride (DAB) solution. Counter-staining was performed with Gill's hematoxylin.

For immunofluorescent double staining for H^+/K^+-ATPase and AQP4, primary antibody reaction was performed in a way similar to that described above. Immunoreactivity was detected using Alexa Fluor 568 goat anti-mouse IgG and 488 goat anti-rabbit IgG (1:1000, Molecular Probes, OR, USA).

For morphometric analysis of H^+/K^+-ATPase, AQP4, or KCNQ1-positive cells, ten randomly chosen micrographs of the gastric fundic glands (50 μm wide from the bottom of the glands to the mucosal surface) were obtained from each immunostained specimen, and the mean numbers of H^+/K^+-ATPase-, AQP4-, or KCNQ1-positive cells on the micrographs were compared between the LPZ-treated and the control mice.

Western Blotting

Liquid nitrogen frozen specimens of the stomach were homogenized in ice-cold RIPA Buffer (Upstate, Temecula, CA, USA) containing protease inhibitor cocktail (Sigma Chemical Co., St. Louis, MO), incubated on ice for 30 min, and centrifuged at 10,000 × *g* for 15 min; supernatant was used for the experiments. The total protein concentration was measured with the BCATM Protein Assay kit (PIERCE, Rockford, IL, USA). Proteins were separated by 12.5% NuPAGE Bis-Tris gel (Invitrogen, CA, USA) electrophoresis using MOPS running buffer (Invitrogen) in the presence of an antioxidant reagent (Invitrogen). Proteins were then transferred onto polyvinylidene difluoride membranes (Invitrogen). Blots were blocked with a solution containing Block Ace (Dainippon Sumitomo pharma Co., Osaka, Japan) for 1 h at room temperature and probed with anti-AQP4 antibody (AB3068, 1:1000, Chemicon, CA, USA) followed by reprobing with anti-β-actin antibody (1:20000, clone: AC-74, Sigma) as the loading control. Signal detection of the positive bands was facilitated by enhanced chemiluminescence assay using ECL plus (GE Healthcare, Uppsala, Sweden). Band quantitation was performed using the ImageJ program (National Institutes of Health, Maryland, USA).

RNA Purification and Quantitative RT-PCR Analysis

Total RNA was extracted from each stomach tissue specimen using the RNeasy Mini Kit (Qiagen, CA, USA) and DNase treatment was performed with an RNase-free DNase kit (Qiagen). RNA was converted into cDNA using the PrimeScript RT reagent kit (Takara, Ohtsu, Japan). The cDNA was diluted ten-fold and used for quantitative PCR analysis with Dice (Takara) using SYBR Premix Ex TaqII (Takara). The mRNA expressions of mouse AQP4, KCNQ1, H^+/K^+-ATPase α subunit (ATP4a), Shh, Muc6, pepsinogen C, and β-actin were measured. The primer sequences are shown in Supplemental Table S1. Data for each gene were normalized to the expression level of β-actin.

Statistical Analysis

All the data were expressed as mean ± standard error. Statistical significance of the differences between two groups was evaluated using unpaired Student's *t* test. All the statistical analyses were performed using SPSS software for Windows, version 17.0J (SPSS Japan, Tokyo, Japan). A two-sided p value of <0.05 was considered as denoting statistical significance.

Results

PPI Administration Induced Mucosal Hyperplasia with Multiple Cystic Dilatations

The gastric mucosal surface pH was higher in the LPZ-treated mice ($n = 10$) than in the control mice ($n = 11$)

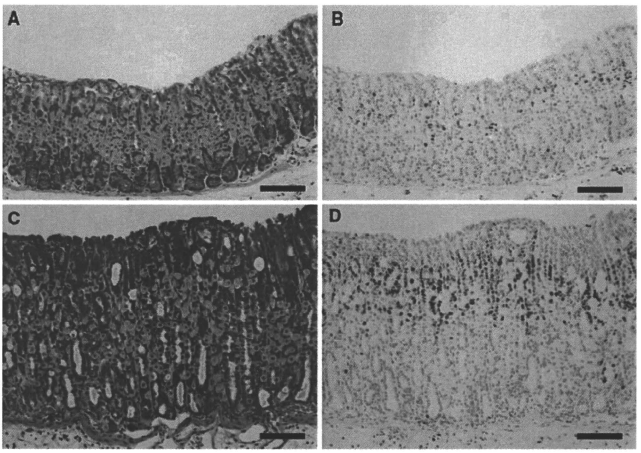

Fig. 1 Hyperplasia with multiple cystic dilatations after PPI administration. **a** Representative histology (H&E stain) in the control mouse. **b** Representative immunohistochemistry for Ki67 in the control mouse; Ki67-positive cells are localized in the proliferative zone at the neck region of the fundic glands. **c** Representative histology (H&E stain) in the LPZ-treated mouse; gastric mucosal hyperplasia with multiple cystic dilatations are observed. **d** Representative immunohistochemistry for Ki67 in the LPZ-treated mouse; Ki67-positive cells are observed widely in the isthmus and neck region of the fundic glands (×200, *bars* = 100 μm)

(LPZ 6.7 ± 0.1; Cont. 3.4 ± 1.7; $p = 0.002$). Serum gastrin levels were also higher in the LPZ-treated mice than in the control mice (LPZ 285 ± 40 pg/ml; Cont. 184 ± 26 pg/ml; $p = 0.049$).

The results of the histological analysis revealed gastric mucosal hyperplasia with multiple cystic dilatations in eight of 10 LPZ-treated mice, although no polyp formation could be observed (Fig. 1c). Inflammatory cell infiltrations in the submucosa and lamina propria were not observed. The number of Ki67-positive cells was significantly increased in the LPZ-treated mice compared to that in the control mice (Fig. 1b, d), suggesting that LPZ administration induced gastric mucosal hyperproliferation.

Disturbed Parietal Cell Differentiation After PPI Administration

The results of immunohistochemical analysis revealed that, in the control mice, AQP4-positive parietal cells were localized in the basal region (Fig. 2b). The KCNQ1-positive parietal cells were distributed at a slightly lower level than the H^+/K^+-ATPase-positive parietal cells in the fundic glands (Fig. 2a, c). This finding is consistent with the results of the previous study, which showed that H^+/K^+-ATPase-specific signal was stronger in parietal cells from the upper part of the fundic glands, and KCNQ1 expression is stronger in the basal parietal cells [34]. On the other hand, in the LPZ-treated mice, the distribution of AQP4-positive parietal cells extended upward to the neck region of the fundic glands (Fig. 2e). A significant increase in the number of KCNQ1-positive parietal cells was observed in the LPZ-treated mice (Fig. 2f). The results of morphometric analysis also supported the findings of the significant increase in the number of AQP4- positive parietal cells and KCNQ1-positive parietal cells (Fig. 2h, i), while the number of H^+/K^+-ATPase-positive parietal cells was not significantly different between the LPZ-treated mice and the control mice (Fig. 2g).

The results of immunofluorescent double staining for AQP4 and H^+/K^+-ATPase revealed that AQP4 was expressed predominantly on the basolateral membrane of the parietal cells in the lower part of the fundic glands (Fig. 3a). In the LPZ-treated mice, the extension of AQP4-positive parietal cells towards the neck region of the fundic glands is clearly observed. H^+/K^+-ATPase-positive parietal cells became smaller in size after LPZ treatment.

Taken together, PPI administration induced the alteration of the distribution of AQP4-positive parietal cells, and increased the number of both AQP4-positive cells and KCNQ1-positive cells in the fundic glands. These results suggest the disturbance of parietal cell differentiation.

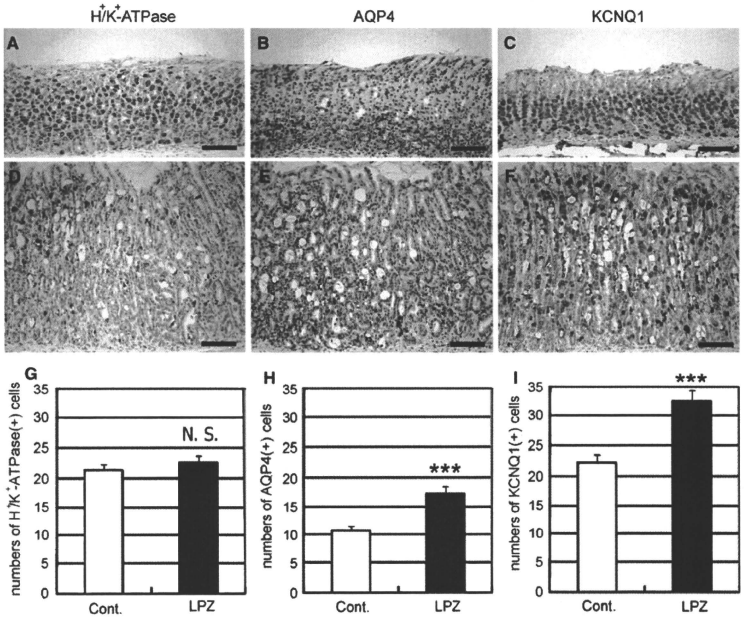

Fig. 2 Impaired parietal cell differentiation after PPI administration. **a** Representative immunohistochemistry for H^+/K^+-ATPase in the control mouse; H^+/K^+-ATPase-positive parietal cells are observed in the isthmus and neck region of the fundic glands. **b** Representative immunohistochemistry for AQP4 in the control mouse; AQP4-positive parietal cells are mainly localized in the lower part of the fundic glands. **c** Representative immunohistochemistry for KCNQ1 in the control mouse; KCNQ1-positive parietal cells are observed in the isthmus and neck region of the fundic glands. The KCNQ1-positive parietal cells were distributed at a slightly lower level than the H^+/K^+-ATPase-positive parietal cells in the fundic glands. **d** Representative immunohistochemistry for H^+/K^+-ATPase in the LPZ-treated mouse; the distribution of H^+/K^+-ATPase-positive parietal cells extend to the entire length of the fundic glands. **e** Representative immunohistochemistry for AQP4 in the LPZ-treated mouse; the distribution of AQP4-positive parietal cells extends towards the neck region of the fundic glands are observed. **f** Representative immunohistochemistry for KCNQ1 in the LPZ-treated mouse; the distribution of KCNQ1-positive parietal cells extend to the entire length of the fundic glands (×200, *bars* = 100 μm). **g–i** Morphometric analysis of H^+/K^+-ATPase, AQP4 or KCNQ1-positive parietal cells; significant increase in the mean numbers of both AQP4-positive parietal cells and KCNQ1-positive parietal cells are observed in the LPZ-treated mice, while the mean number of H^+/K^+-ATPase-positive parietal cells is not different between in the LPZ-treated mice and in the control mice (means ± SE, *** $p < 0.001$, $n = 10$ LPZ-treated mice, $n = 11$ control mice)

Increased Expression of AQP4 and KCNQ1 and Decreased Expression of Sonic Hedgehog in the Gastric Parietal Cells After PPI Administration

The result of Western blotting revealed that the gastric mucosa of the LPZ-treated mice exhibited a higher expression level of the AQP4 protein than that of the control mice (Fig. 4). The expression level of the AQP4 mRNA also increased in the LPZ-treated mice (Fig. 5a). In addition, the expression of KCNQ1 mRNA tended to be increased in the LPZ-treated mice ($p < 0.1$; Fig. 5b). The expression of KCNQ1 mRNA was correlated with that of AQP4 mRNA in the LPZ-treated mice, but not in the controls (Fig. 5c, d). Moreover, the mRNA expression of Shh, which is also expressed in the parietal cells, was decreased in the LPZ-treated mice as compared with that in the control mice (Fig. 5f). However, no significant difference in the expression of H^+/K^+-ATPase mRNA was noted between the LPZ-treated and control mice (Fig. 5e).

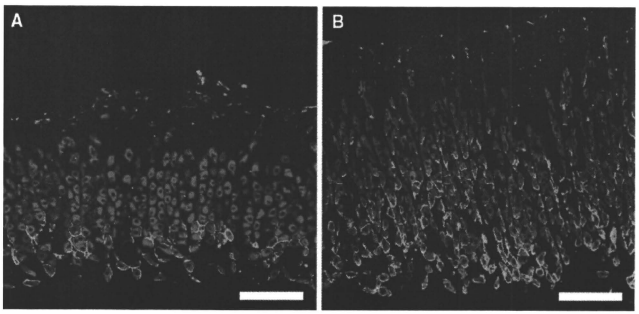

Fig. 3 Immunofluorescent double staining for AQP4 and H^+/K^+-ATPase. **a** Representative immunofluorescence for AQP4 and H^+/K^+-ATPase in the control mouse; AQP4 is expressed on the basolateral membrane of the parietal cells in the lower part of the fundic glands (AQP4-positive parietal cells). **b** Representative immunofluorescence for AQP4 and H^+/K^+-ATPase in the LPZ-treated mouse; the extension of AQP4-positive parietal cells towards the neck region of the fundic glands is clearly observed. H^+/K^+-ATPase-positive parietal cells become smaller in size (×200, *bars* = 100 μm)

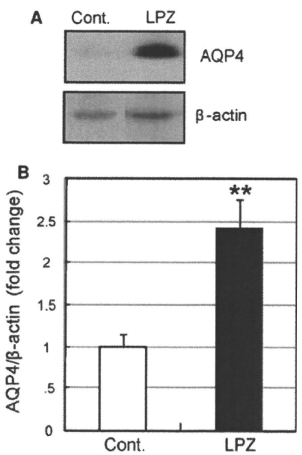

Fig. 4 Increased expression of AQP4 protein after PPI administration. **a** The protein expression level of AQP4 was analyzed by Western blotting in the LPZ-treated mice and the control mice. β-actin was used as the loading control. **b** Band quantitation for the results of Western blotting; significantly increased expression of the AQP4 protein was observed in the LPZ-treated mice (means ± SE, ** $p < 0.01$, $n = 10$ LPZ-treated mice, $n = 11$ control mice)

Delayed Mucous Neck-to-Zymogenic Cell Differentiation After PPI Administration

In normal fundic gland, the mucous neck cells secrete Muc6 and pepsinogen. As mucous neck cells migrate towards the bases of fundic glands, they transdifferentiate into zymogenic cells, which do not secrete Muc6 but continue to secrete pepsinogen in abundance [35, 36]. In the present study, while Muc6-positive cells were strictly localized to the neck region of the fundic glands in the control mice (Fig. 6a), Muc6-positive cells were detected even in the basal region of the fundic glands in the LPZ-treated mice (Fig. 6c). On the other hand, while the pepsinogen-positive cells were mainly localized to the lower region of the fundic glands in the control mice (Fig. 6b), pepsinogen-positive cells were observed even in the neck region of the fundic glands in the LPZ-treated mice (Fig. 6d). The number of cells co-expressing Muc6 and pepsinogen seemed to be increased at the base of the fundic glands. The results of quantitative RT-PCR revealed that Muc6 mRNA expression was significantly increased (Fig. 6e), while pepsinogen mRNA expression was significantly decreased (Fig. 6f) in the LPZ-treated mice. These results suggest that zymogenic cell differentiation was disrupted, and mucous neck cells, co-expressing Muc6 and low amount of pepsinogen, were increased after PPI administration.

Discussion

In the present study, the PPI-treated mice exhibited striking changes in the components of the epithelial lining of the gastric fundic glands. Although a number of previous studies have reported that PPI treatment leads to mucosal hyperplasia with hypergastrinemia [37–39], mucosal cystic dilatation has not been mentioned yet. However, similar hyperplastic change is also observed in H_2R-null mice [40],